Molecular and Cellular Endocrinology 557 (2022) 111751

Contents lists available at ScienceDirect

Molecular and Cellular Endocrinology

journal homepage: www.elsevier.com/locate/mce

# Transcriptional networks underlying a primary ovarian insufficiency disorder in alligators naturally exposed to EDCs

Matthew D. Hale [a,b,c], Therese Koal [d], Tuan Hai Pham [d], John A. Bowden [e], Benjamin B. Parrott [a,b,*]

[a] Eugene P. Odum School of Ecology, University of Georgia, Athens, GA, USA
[b] Savannah River Ecology Laboratory, University of Georgia, Aiken, SC, USA
[c] Department of Biology, University of Virginia, Charlottesville, VA, USA
[d] Biocrates Life Science Ag, Innsbruck, Austria
[e] Center for Environmental and Human Toxicology, Physiological Sciences, College of Veterinary Medicine, University of Florida, Gainesville, FL, USA

ARTICLE INFO

*Keywords:*
Endocrine disruptors
Ovary
Alligator
Environmental health

ABSTRACT

Interactions between the endocrine system and environmental contaminants are responsible for impairing reproductive development and function. Despite the taxonomic diversity of affected species and attendant complexity inherent to natural systems, the underlying signaling pathways and cellular consequences are mostly studied in lab models. To resolve the genetic and endocrine pathways that mediate affected ovarian function in organisms exposed to endocrine disrupting contaminants in their natural environments, we assessed broad-scale transcriptional and steroidogenic responses to exogenous gonadotropin stimulation in juvenile alligators (*Alligator mississippiensis*) originating from a lake with well-documented pollution (Lake Apopka, FL) and a nearby reference site (Lake Woodruff, FL). We found that individuals from Lake Apopka are characterized by hyperandrogenism and display hyper-sensitive transcriptional responses to gonadotropin stimulation when compared to individuals from Lake Woodruff. Site-specific transcriptomic divergence appears to be driven by wholly distinct subsets of transcriptional regulators, indicating alterations to fundamental genetic pathways governing ovarian function. Consistent with broad-scale transcriptional differences, ovaries of Lake Apopka alligators displayed impediments to folliculogenesis, with larger germinal beds and decreased numbers of late-stage follicles. After resolving the ovarian transcriptome into clusters of co-expressed genes, most site-associated modules were correlated to ovarian follicle phenotypes across individuals. However, expression of two site-specific clusters were independent of ovarian cellular architecture and are hypothesized to represent alterations to cell-autonomous transcriptional programs. Collectively, our findings provide high resolution mapping of transcriptional patterns to specific reproductive function and advance our mechanistic understanding regarding impaired reproductive health in an established model of environmental endocrine disruption.

## 1. Introduction

Exposure to environmental contaminants that disrupt normal functioning of the endocrine system has broad-scale implications for ecological and human health (Diamanti-Kandarakis et al., 2009; Milnes and Guillette, 2008; Yilmaz et al., 2020; Encarnação et al., 2019; Windsor et al., 2018; Kahn et al., 2020). Epidemiological studies have revealed associations between a wide range of endocrine disrupting chemicals (EDCs) and compromised reproductive health, and lab experiments using rodent models and cell culture have identified potential mechanisms that might underlie these relationships. However, due to the correlative nature of human epidemiology and the environmental decontextualization of rodent and cell culture models, our understanding of the mechanisms and genetic pathways by which EDCs exert biological effects in natural systems remains incomplete. Wildlife exposed to EDCs initially alerted scientists and the public to the consequences of EDC contamination in the environment but were limited due to a lack of analytical and technical resources (Colborn and Thayer, 2000; Guillette and Gunderson, 2001). With the advent of novel computational and genomic approaches, which are capable of providing mechanistic

* Corresponding author. Eugene P. Odum School of Ecology, University of Georgia, Athens, GA, USA.
*E-mail address:* benparrott@srel.uga.edu (B.B. Parrott).

https://doi.org/10.1016/j.mce.2022.111751
Received 3 June 2022; Accepted 3 August 2022
Available online 11 August 2022

insights across the animal kingdom, studies of exposed wildlife are once again poised to advance our understanding of the consequences of EDC exposure by combining environmental relevance with experimental tractability.

The alligator population inhabiting Lake Apopka (Orange County, FL, USA) is exposed to a mixture of EDCs and individuals display a spectrum of reproductive abnormalities including altered levels of circulating sex steroids, decreased ovarian follicle numbers, and extensive dysregulation of the ovarian transcriptome (Guillette, 1994; Moore et al., 2011, 2012a; Hale et al., 2019; Hale and Parrott, 2020). In addition, the ovarian response to gonadotropin signaling is impaired in alligators from Lake Apopka. For example, when challenged with exogenous follicle-stimulating hormone (FSH), ovaries from alligators originating from a reference site display a robust, dose-dependent increase in aromatase expression, whereas this response in Lake Apopka alligators is severely abated (Moore et al., 2010a, 2012a). Studies in fish and mammals have also reported that exposure to EDCs is associated with compromised ovarian responses to gonadotropin signaling, suggesting that an impaired ovarian response to gonadotropin signaling is a conserved hallmark of EDC exposure (Bloom et al., 2017; Rivera et al., 2015; Mahalingaiah et al., 2012; McCoy et al., 2017; Alviggi et al., 2018; Pierron et al., 2014). Despite being fundamental to reproductive health, our understanding of the affected genetic pathways that underlie impaired ovarian responses to pituitary-derived gonadatropin signals remains poor.

Recent reports demonstrate that many of the reproductive perturbations, including the abated response to gonadotropin challenge observed in Lake Apopka alligators, originate during development and are likely to result from maternally-derived contaminant deposition in the yolk (Hale et al., 2019; Hale and Parrott, 2020). The developmental origins and persistent nature of these phenotypes have been isolated in juvenile alligators through experimental designs subjecting field-collected eggs from different populations to identical incubation and post-hatching conditions (i.e., common gardens) and have identified steroidgenic, cellular, and transcriptional abnormalities using targeted approaches. Here, we use a similar experimental design coupled with an exogenous gonadotropin challenge to identify the transcriptional, cellular, and endocrine response to FSH signaling in the alligator ovary. Furthermore, we compare these responses in alligators from Lake Apopka and a nearby reference site to reveal novel genetic pathways that are associated with EDC exposure. However, in order provide a novel, holistic view of reproductive abnormalities Lake Apopka alligators and the linkages between its components, we employ an integrative methodology to query the entire ovarian transcriptome, 17 steroid hormones, and ovarian cellular architecture in FSH-challenged and non-challenged alligators. Then, to identify associations between each of these components, we employ network-based gene clustering analyses to identify cohorts of genes that covary with steroid hormone levels and cellular architecture.

Based on previous reports, we hypothesized that ovarian transcriptomes in Lake Apopka alligators would broadly diverge from those in reference animals, both in the presence or absence of exogenous FSH signals. Further, after deconstructing ovarian transcriptomes into correlated modules comprised of co-expressed genes, we hypothesized that specific modules could be parsed with respect to their association with specific follicle phenotypes and a panel of 17 circulating steroid hormones, and that these modules would provide mechanistic insight into the etiology of the "Apopka Reproductive Phenotype." Collectively, this study is aimed at advancing our understanding of the mechanistic links between EDC-associated reproductive perturbations in natural populations.

## 2. Methods

### 2.1. Animal husbandry and sample collection

All experiments and analyses employed in this study were reviewed and approved by the Institutional Animal Care and Use Committee of the Medical University of South Carolina (Charleston, SC). American alligators (*Alligator mississippiensis*) were collected as eggs, permitted by the Florida Fish and Wildlife Conservation Commission. Descriptions of alligator egg collections and husbandry employed herein are available in prior studies (Hale et al., 2019; Hale and Parrott, 2020; Galligan et al., 2019). In brief, alligator eggs were collected from two sites in central Florida, Lake Apopka (AP) and Lake Woodruff National Wildlife Refuge (WO; Volusia County, FL). AP is a site characterized historically by organochlorine pesticide (OCP) contaminant input including DDT and metabolites, and these contaminants and others have been reported at elevated levels in resident juvenile and adult alligator tissues in addition to egg yolk (Guillette, 1994; Guillette et al., 1999; Heinz et al., 1991; Rauschenberger et al., 2007, 2009). In contrast, WO is a relatively undisturbed site for which little-to-no direct contaminant input has been described and is used herein as a reference site. Embryos were collected as eggs from both WO and AP in June 2014 shortly after oviposition, were candled to assess viability, and susbequently transferred to artificial nests of damp sphagnum moss, where they were maintained at 32 °C. From AP, 18 eggs were collected in total from 5 individual clutches; 15 eggs total from 11 clutches were collected from WO. One additional egg was staged from each clutch according to Ferguson (Ferguson et al., 1985); all eggs were collected at or prior to stage 16, which precedes the differentiation of the bipotential gonad (stage 21). Alligators used in this study were collected as part of a larger investigation into reproductive developmental impacts of early-life exposures to exogenous estrogens; all animals in the current study received a topical vehicle (95% ethanol) as stage 19 embryos. Stage 21 is the earliest stage at which the developing gonad begins to differentiate into male- or female-specific structures.

Upon reaching stage 19, which precedes sex determination and gonadal differentiation, embryos were incubated at 30 °C, a temperature that exclusively produces females. Hatchlings were maintained in indoor fiberglass tanks at the Hollings Marine Laboratory on 12/12 light dark cycles and were individually marked with unique numbered monel tags affixed between the middle digits of both hindlimbs. For approximately two months after hatching, all neonates were fed *ad libitum* with a commercial croc chow (Mazuri Exotic Animal Nutrition). Once individual disparities in size and growth became apparent, animals were weighed and sorted every two weeks according to size, ensuring that similarly sized individuals were housed together. At two months of age, animals were switched to a feeding schedule according to size: smallest animals (<92 g) were fed daily, intermediate animals (92–132 g) were fed three times weekly, and largest animals (>132 g) were fed twice weekly. At approximately five months of age, all animals from both AP and WO were divided into two treatment groups and received 4 daily consecutive intramuscular injections at the base of the tail of either 277 μU/g body weight recombinant ovine FSH ("FSH"; Sigma-Aldrich F8174, St. Louis, MO) or 0.8% sterile saline vehicle control ("VEH"). Animals were euthanized on the fifth day after initial injections with 0.1 mg/g pentobarbital (Sigma-Aldrich, St. Louis, MO), followed by decapitation. Ovaries were immediately dissected, weighed, and fixed. Right ovaries were fixed in RNAlater, rocked 12–16 h at 4 °C, and stored at −80 °C. Left ovaries were fixed for 24 h in 10% NBF, rinsed, and stored at 4 °C in 70% ethanol. Total RNA was isolated from ~10 mg of ovarian tissue. Crocodilian ovaries exhibit regional structural diversity

(i.e., the medullary rest (Forbes, 1939; Moore et al., 2010b)), thus care was taken to extract RNA from a medial transverse section of each ovary. Extractions were performed using an AGPC extraction protocol utilizing column-purification and on-column DNase I digestion (Hale and Parrott, 2020).

### 2.2. Transcriptomic response to FSH challenge

To sequence transcriptomes, stranded libraries were generated from *A. mississippiensis* total ovarian RNA (1–2 μg; extractions outlined above) following poly(A)-enrichment (KAPA Stranded mRNA-Seq Kit; KAPA Biosystems; Cape Town, South Africa) and sequenced on an Illumina NextSeq (75bp PE; 150 cycles total). Seven libraries were sequenced for each pairwise combination of site and FSH (AP-FSH, AP-VEH, WO-FSH, WO-VEH; 28 libraries total). Resulting reads were assessed for quality via FastQC (http://www.bioinformatics.bbsrc.ac.uk/projects/fastqc) and MultiQC (Ewels et al., 2016). All reads exhibited mean phred scores >30 and did not contain adapter sequence contamination, thus were not subjected to quality trimming. Reads were aligned to the *Alligator mississippiensis* genome assembly ASM2811v4 using Hisat2 (2.1.0) (Kim et al., 2015); read counts were generated from resulting alignments using R packages 'GenomicFeatures' and 'GenomicAlignments' (Lawrence et al., 2013) (parameters: mode = "Union"; singleEnd = FALSE, ignore.strand = FALSE, fragments = TRUE).

Differential gene expression analysis was conducted using R (R Core Team; www.R-project.org; version 1.1.456) package edgeR (Chen et al., 2016; McCarthy et al., 2012; Robinson et al., 2009; Robinson and Smyth, 2007). Genes with expression below 1 count per million (CPM) and expressed in fewer than seven libraries were removed, retaining 18,435 genes for analysis. Two libraries from the WO-FSH group were removed from the study as outliers due to high biological coefficient of variation (BCV) values and abnormally low follicle counts (n = 5 libraries after outlier removal; 26 libraries total) (Hale and Parrott, 2020). Filtered read counts for remaining libraries were TMM-normalized and fit to a quasi-likelihood negative binomial model using edgeR function 'glmQLFit' (robust = TRUE). Genewise statistical testing was carried out using quasi-likelihood F-tests via edgeR function 'glmQLFTest' for planned linear contrasts investigating responses within each population to gonadotropin stimulation (e.g., AP-FSH vs AP-VEH). Significant changes in expression between groups were identified using a Benjamini-Hochberg adjusted p-value ("FDR") < 0.05. Changes in FSH-responsive gene cohorts were identified using presence/absence comparisons of differentially expressed genes across populations.

A relatively large proportion of genes assessed herein are uncharacterized loci in alligator genome (5469 of 18,435 total genes passing filtering). Many of these loci are functionally relevant to the ovary (e.g., *CYP19A1* [LOC102566432], *CYP17A1* [LOC102567971], and *CYP11A1* [LOC102569028]), thus we sought to provide secondary evidence as to their identity in a systematic fashion. Briefly, we used a two-pass transcriptome assembly to generate putative alligator transcripts in StringTie (Pertea et al., 2015, 2016) using alligator RefSeq annotations (GCF_000281125.3, annotation release 102) as a guide. Fasta sequences from the resulting assembly were extracted using GFFread (Trapnell et al., 2010) and blasted (Blastx) against the Uniprot Swiss-prot database (Apweiler et al., 2004) with an e-value cutoff = $1e^{-5}$. Annotation evidence for uncharacterized loci were taken from top-hits according to e-value and gene names were used in place of 'LOC' identities in downstream analyses. Any LOC loci not identified by this approach was excluded from further analysis beyond testing for differential expression. This method identified 2666 of 5469 expressed LOC loci.

### 2.3. Ovarian histology and follicle, germ cell bed morphology

Right ovaries fixed in 10% NBF were bisected horizontally along the transverse midline into two equal halves and paraffin embedded for sectioning at 4 μm thickness, yielding two cortical cross sections per ovary per section. Sections were stained with hemotoxylin and eosin and imaged using a Keyence BZ-X710 microscope at 10× and 20× magnification. Serial images were taken for each section and composite stitched using Keyence automated stitching software. Resulting images were analyzed in ImageJ; total cortical area was measured using the freehand selection tool and by tracing the distinct border separating the ovarian cortex from underlying medulla and lacunae. Intracortical trabeculae were identified and subtracted from total cortical area. Stage III follicles (SIII) were identified by their large size, distinct pink, basophilic cytoplasm, and by the presence of a complete layer of follicular granulosa cells surrounding each oocyte. Germ cell beds were identified last, after clearly demarcating sIII follicles and trabeculae, as these landmarks help define their borders. Nuclear characteristics were used to first identify individual oocytes; stage I (sI), or primary, and stage II (sII) oocytes exhibit spherical nuclei and can frequently be multinucleated, contrasting with ovoid or oblong nuclei of somatic cells (Moore et al., 2008, 2010b). Clusters of oocytes, or beds, were then distinguished from one another by intervening trabecular tissue or by larger sIII follicles (Moore et al., 2008, 2010b). Following identification, the area of the individual germ cell beds and sIII follicles was measured using the freehand selection tool. Density of oocytes and somatic cells within beds was assessed by counting nuclei for each cell type (large spherical oocyte nuclei and small oblong somatic cell nuclei) and dividing by corresponding bed area. This process was conducted for three randomly selected beds in each cortical section and cell densities were averaged across beds. If a given section had fewer than three observable beds, counts were made and averaged for all available beds. Where possible, sections from both halves of an ovary were assessed and averaged. Differences in sIII and bed area proportion, bed density per unit area cortex, germ cell density per unit area bed, and total cortical area were assessed via 2-way ANOVA with main effects of site (AP, WO) and FSH treatment (FSH, VEH). Post-hoc analyses were used where significant main effects were observed (alpha = 0.05) via Sidak's multiple comparisons test.

### 2.4. Population and gonadotropin effects on circulating steroid hormone levels

Circulating hormone levels were quantified in alligator plasma samples collected both at the onset (PRE) and conclusion (TOD) of the four-day FSH challenge period in vehicle (VEH) and FSH-treated individuals, permitting repeated-measures analysis (described below). Seventeen steroid hormone species were isolated from plasma using solid-phase extraction and quantified via UPLC™-MS/MS (Waters Acquity I-Class/Xevo® TQ-S micro system; Waters, Vienna, Austria) using an AbsoluteIDQ® Stero17 Kit (Biocrates Life Sciences AG; Innsbruck, Austria) (Koal et al., 2012; Bae et al., 2021). This approach permitted parallel quantification of 17 steroid hormones, including: cortisol, cortisone, 11-deoxycortisol, corticosterone, 11-deoxycorticosterone, 17a-hydroxyprogesterone, progesterone, aldosterone, estradiol, estrone, androstenedione, androsterone, dehydroepiandrosterone (DHEA), dehydroepiandrosterone sulfate (DHEA-S), dihydrotestosterone (DHT), etiocholanolone, and testosterone. Data processing and hormone concentration determination were conducted using MetIDQ™ software (version 'Carbon'; Biocrates).

Differences in circulating hormone levels were assessed using mixed-effects linear models via package 'nlme' in RStudio; concentrations were transformed as necessary to achieve residual normality and were regressed against main effects of site (AP, WO) and FSH-treatment group (FSH, VEH). Collection time point (PRE, TOD) was also included as a main effect. Individual sample ID was included as a random effect to account for repeated measures. Where homoscedasticity could not be achieved via transformation, argument 'weights = varIdent (from = ~1| group)' was used in nlme to account for whichever main effect drove differences in variance. In instances were analyte concentrations fell below the limit of detection (LOD), one half of LOD (0.5 * LOD) was

substituted in its place. Where significant main effects of either site or FSH treatment group were detected (alpha = 0.05), Mann-Whitney U tests were used post-hoc to identify differences between treatment levels (e.g., AP-VEH versus WO-VEH [site effect] or AP-VEH versus AP-FSH [FSH effect]).

### 2.5. Transcription factor and Gene Ontology (GO) enrichment

Enrichment of transcription factors (TFs) in regulating ovarian responses to FSH was conducted using Enrichr (Chen et al., 2013; Xie et al., 2021; Kuleshov et al., 2016) with significantly differentially expressed genes between FSH treatment groups (VEH vs FSH). Significantly enriched terms were identified separately for DEGs upregulated and downregulated in FSH-treated animals relative to VEH-treated animals using an adjusted p-value threshold (adj. $p < 0.05$). Enrichment analysis was carried out in two independent experiments: the first identified enriched TFs in all positively- and negatively-regulated FSH DEGs in WO animals including DEGs shared with responses in AP animals; the second identified enriched TFs in DEGs that were exclusive to AP animals (i.e., DEGs unique to AP).

Gene ontology (GO) enrichment of network module genes (described below) was conducted using g:Profiler (Reimand et al., 2016). Prior to analysis, alligator gene identifiers were converted to human Ensembl gene ids (ENSG). Any redundant term identified within a given module after ENSG conversion was reduced to a single occurrence, so no duplicates occurred. Enrichment was conducted against an alligator ovarian-specific background comprised initially of all 18,435 genes passing expression filtering in DEG analyses. Following ENSG conversion and de-duplication, 13,542 background genes were used for enrichment testing of GO:BP terms in network module member genes against only background genes with annotations. Significantly enriched pathways were identified using a multiple testing correction adjusted p-value (adj. $p < 0.05$; method g:SCS (Reimand et al., 2016)).

### 2.6. Weighted gene Co-expression network analysis and trait associations

A network-based approach through WGCNA (Langfelder and Horvath, 2008) ("weighted gene co-expression network analysis) was employed to delineate clusters of highly correlated genes, or co-expression modules, in the ovarian transcriptome. Then, to elucidate how these clusters may be driven by or contribute to altered phenotypic traits, we employed principal components analysis to generate eigengenes (PC1) as summarized expression patterns for each module in WGCNA; linear modeling was subsequently used to screen module eigengenes for relationships to traits. Traits assessed included site (WO, AP), ovarian cellular architecture, and plasma androgen levels (testosterone, androstenedione, and etiocholanolone). As we have previously used correlative methods to identify strong associations between sIII follicle number and divergent ovarian transcriptional patterns across site (Hale and Parrott, 2020), herein we focused instead on the proportion of ovarian cortical area occupied by germ cell beds (bed area proportion). Finally, we also assessed if eigengenes were significantly associated with gonadotropin stimulation (FSH/VEH).

Network analysis of gene expression was conducted using R package WGCNA (Langfelder and Horvath, 2008) on vst-transformed (variance stabilizing transformation) (Love et al., 2017) read counts for all genes passing low-expression filtering in 26 non-outlier libraries. Prior to transformation, read counts across all samples were normalized via a "median of ratios" approach to account for differences in library size and RNA composition, as implemented in package DESeq2 (Love et al., 2014). Pairwise Pearson correlations were calculated for filtered-normalized- transformed read counts to generate a signed network using WGCNA function blockwiseModules (parameters: soft threshold = 17; pamStage = TRUE; pamRespectsDendro = TRUE; mergeCutHeight = 0.15; minModuleSize = 30; maxBlockSize = 18435), yielding a network comprised of 12 co-expression modules and one orphan "module" of unassigned genes. Principal components analysis was used to extract eigengenes (PC1) for each module. Statistical associations between module eigengenes and trait values were assessed via linear modeling using RStudio function 'lm' for main effects of site, FSH, bed area proportion (of total cortical area), and plasma testosterone, androstenedione, and etiocholanolone. Eigengene values were transformed as necessary to achieve normality of residuals and homoscedasticity, as assessed via Shapiro-Wilk and Breusch-Pagan test (alpha = 0.05) respectively. For one module, homoscedasticity could not be achieved via transformation, thus a heteroskedasticity-consistent variance-covariance matrix was estimated for parameters using R package 'sandwich' function vcovHC (type = "HC3"). Hub genes for each module were determined using WGCNA function 'chooseTopHubInEach Module'.

## 3. Results

### 3.1. Transcriptional responses to gonadotropin stimulation

To describe regulation of ovarian function by gonadotropins in the alligator, we first sought to characterize FSH-responsive gene cohorts in both WO and AP populations (Fig. 1). Both populations exhibited distinct transcriptional responses to FSH stimulation, including canonical FSH-regulated genes aromatase (CYP19A1), inhibin subunit-α (INHA), and follistatin (FST). However, substantially more genes were found to be responsive in AP animals than WO (Fig. 2A). In WO alligators, 1965 genes were significantly upregulated by FSH treatment while 248 were suppressed. Of these FSH-responsive genes in WO ovaries, 76.4% (1690/2213) were shared when compared to AP (Fig. 2B). In contrast, alligators from AP exhibited a more robust response to FSH, with the number genes both positively and negatively affected by FSH stimulation approximately three-fold greater relative to WO (6,036 vs. 2,213, respectively). This general pattern was also apparent at the level of the entire transcriptome (all expressed genes; not limited to DEGs). The median abs ($\log_2$ [fold change]) between VEH and FSH-treated groups was significantly higher at AP compared to WO (Fig. 2B; AP median = 0.2799; WO median = 0.2262; Mann Whitney $p < 0.0001$), indicating a greater magnitude of expression changes occurred between VEH and FSH treated animals at AP compared to WO.

Consistent with observed population-specific responses, unique subsets of transcription factors (TFs) were associated with up and downregulated genes in each population (Fig. 2C). In transcriptomes of WO alligator ovaries, 56 distinct TFs were significantly enriched (adjusted $p < 0.05$) as likely regulators of those genes upregulated by FSH. Most highly enriched factors included: Erythroid Krueppel-like Factor (EKLF); MYC proto-oncogene, bHLH transcription factor (MYC); and cAMP-responsive element modulator (CREM), as well as the epigenetic regulator lysine demethylase 5b (KDM5B) and Clock circadian regulator (CLOCK) (Fig. 2C; Table S1 "WO_FSH_Up_All" (Hale and Parrott, 2022)). In contrast to genes upregulated by FSH, relatively few TFs (9 total) were enriched for genes downregulated by FSH in WO animals. Enriched factors included hepatocyte nuclear factor 4 alpha (HNF4a); catenin beta 1 (CTNNB1); E74-like ETS transcription factor 3 (ELF3); and melanocyte inducing transcription factor (MITF). The pioneer TF Forkhead Box A1 (FOXA1) and lysine demethylase 2B (KDM2B) were also among enriched TFs in downregulated genes (Fig. 2C; Table S2 "WO_FSH_Down_All" (Hale and Parrott, 2022)). Only one TF was shared between these groups, Wilms-Tumor 1 (WT1), suggesting that largely unique cohorts of transcriptional regulators are responsible for positive and negative responses to FSH in WO animals.

Genes upregulated by FSH that were unique to AP animals were also highly enriched. Sixty TFs were identified for DEGs upregulated by FSH, many of which (40 total, 66%) were also enriched for upregulated genes at WO. Top amongst shared terms were MYC, CREM, E2F1, EKLF, GABP, and KDM5B (Fig. 2C; Table S3 "AP_FSH_Up_Unique" (Hale and Parrott, 2022)). In contrast, only one TF, WT1, was enriched in both populations

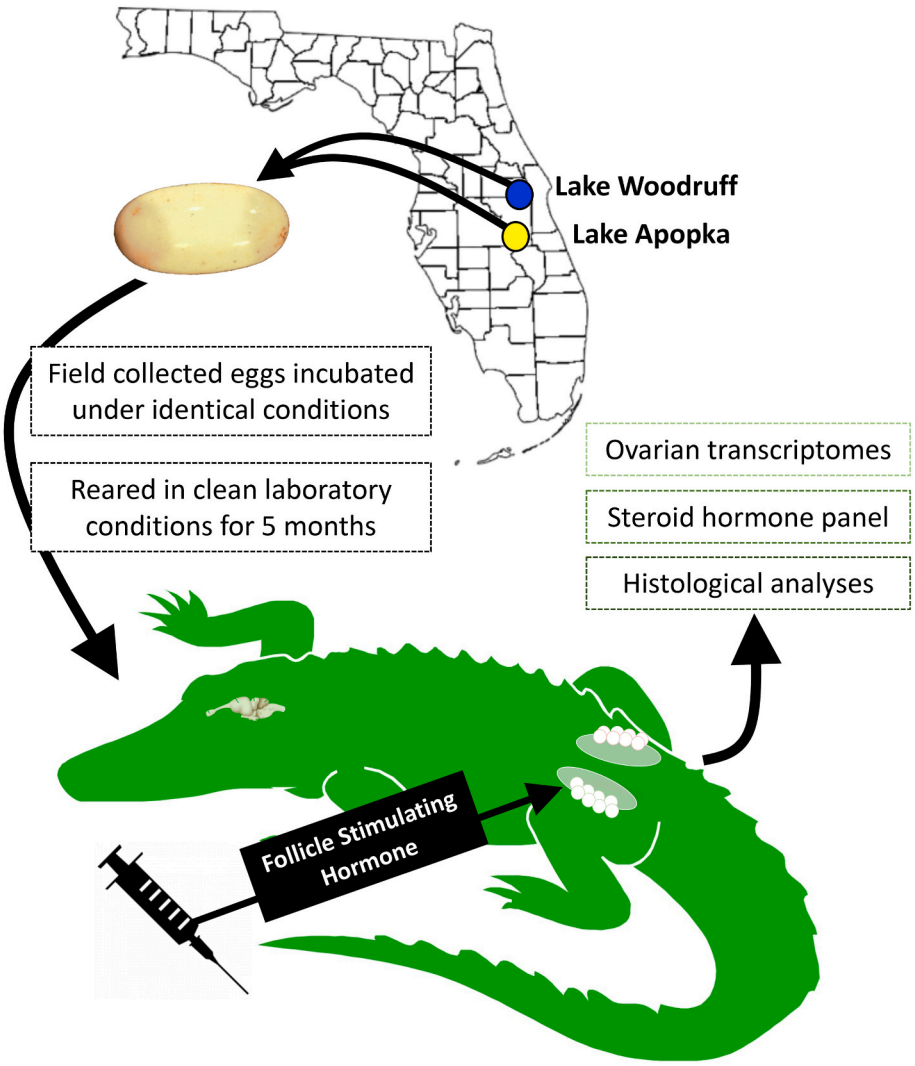


**Fig. 1. Common garden experimental design and FSH challenge.** Alligator eggs were collected from two geographically proximal sites conveying different exposures to EDCs and then incubated under identical conditions. Resulting hatchlings were reared in a laboratory common garden for 5 months and then either treated with follicle stimulating hormone or vehicle. A series of analytical approaches were then employed to resolve connections between circulating levels of steroid hormones, ovarian follicle histology, and ovarian gene expression profiles.

for genes downregulated by FSH. Additional TFs enriched exclusively in AP-unique DEGs included: zinc finger protein 217 (ZNF217), SWI/SNF Related, Matrix Associated, Actin Dependent (SMARCD1), Signal Transducer and Activator of Transcription 3 (STAT3), and Forkhead Box A2 (FOXA2), among others (Fig. 2C; Table S4 "AP_FSH_Down_Unique" (Hale and Parrott, 2022)).

### 3.2. Gonadotropin stimulation of ovarian steroidogenesis

A key function of gonadotropin signaling in the ovary is the stimulation of steroidogenesis, thus we next described possible divergent transcriptional responses to FSH for member genes of the ovarian steroidogenesis pathway (KEGG Pathway: map04913). Both populations responded positively to FSH by upregulating expression of canonical steroidogenic enzymes *CYP17A1* (LOC102567971), *CYP11A1* (LOC102569028), *HSD17B1*, and *CYP19A1* (LOC102566432), as well as *FSHR*, and *PKA* signaling components (PRKACB; Fig. 3; aquamarine boxes), and by downregulating expression of phospholipase A2, *PLA2* (PLA2G4A; Fig. 3; yellow box). In contrast, expression of three members of this pathway exhibited significant differences between VEH and FSH groups that were unique to AP animals. Expression of *COX2* (prostaglandin-endoperoxide synthase 2) and *IGF1R* (insulin-like growth factor 1 receptor) both decreased in AP FSH animals relative to VEH (Fig. 3; yellow starred boxes), while expression *ARTISt*, or *ACOT1*, (acyl-coenzyme A thioesterase 1) was uniquely upregulated in AP FSH animals (blue starred box).

### 3.3. Steroidgenic responses to gonadotropin stimulation

In light of variation in expression of steroidogenic factors in the ovary, we next sought to explore changes in circulating steroid hormone levels in the context of FSH stimulation. In both WO and AP animals, we observed robust increases in circulating estradiol (E2) with FSH stimulation (FSH main effect: $p = 0.001$). This response did not differ between sites (Fig. 4A) however, and E2 was the only hormone assayed that exhibited a significant response to FSH. In contrast, testosterone (T) levels exhibited marginal increases in FSH-treated animals (Fig. 4B), but these effects were not significant ($p = 0.088$). However, T levels were significantly elevated in AP animals relative to WO ($p = 0.004$). Post-hoc analyses confirmed this elevation in both FSH and VEH (control) groups at the pre-challenge time point (WO vs. AP [VEH]: $p = 0.012$, $U = 0$, median difference $= -0.023$; WO vs. AP [FSH]: $p = 0.001$, $U = 0$, median difference $= -0.029$). This observation underscored a general pattern of hyperandrogenism in AP animals; in addition to T, both androstenedione (Fig. 4C; $p = 0.005$) and etiocholanolone (Fig. 4D; $p = 0.005$) were significantly elevated at AP relative to WO. For androstenedione, post-hoc analysis confirmed significant elevation at AP for the pre-challenge time point (WO vs. AP [FSH]: $p = 0.0495$, $U = 9$,

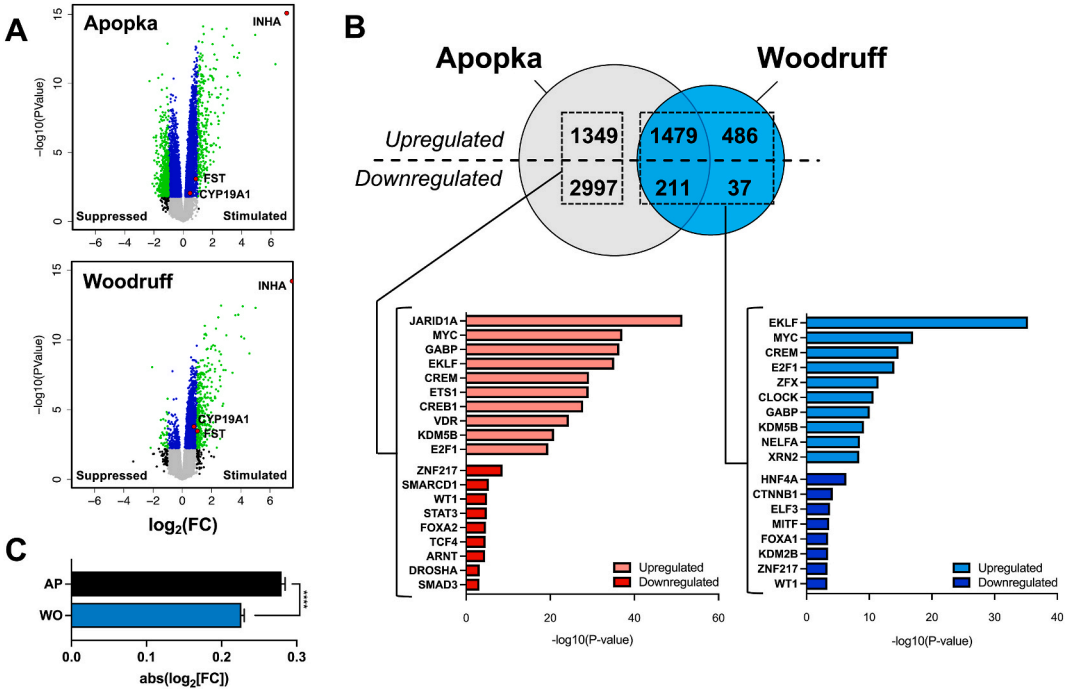


**Fig. 2. Ovarian Transcriptional Responses to Gonadotropin Stimulation.** (A) Volcano plots illustrating the $log_2$(FC) and relative significance of expression differences between VEH and FSH treated WO and AP animals. Both blue and green points are significantly differentially expressed (DEGs) between treatment groups within each population (Apopka, Woodruff), while green points are both significant DEGs and exhibit $log_2$(FC) > |1|. Points with positive $log_2$(FC) values are expressed at higher levels in FSH treated animals relative to VEH, while points with negative $log_2$(FC) are expressed at lower levels in FSH-treated animals. (B) Transcription factor enrichment via Enrichr of DEGs positively and negatively regulated by FSH in both WO (blue bars) and AP (red bars). Enrichment analyses conducted for WO include all genes overexpressed in FSH animals relative to VEH (upregulated) or suppressed in FSH animals relative to VEH (downregulated). Enrichment analyses for AP include genes uniquely overexpressed or suppressed in FSH animals relative to VEH (i.e., genes not also found to be responsive in WO animals). (C) Median absolute value of $log_2$(FC) between VEH and FSH treated animals at AP and WO for all genes passing filtering. Bar and asterisks denote significance as assessed via Mann Whitney non-parametric T-test.

median difference = −0.019). Androstenedione levels were similarly elevated for VEH animals at the pre-challenge time point, as well as for FSH animals at the TOD time point, but these changes were not significant. Lastly, etiocholanolone levels were significantly elevated in AP alligators compared to WO at the pre-challenge time point for both FSH (p = 0.005, U = 3.5, median difference = −0.051) and VEH groups (p = 0.02), U = 6.5, median difference = −0.069), as well as at the TOD time point for FSH groups (p = 0.012, U = 5.5, median difference = −0.015).

Interestingly, expression of HSD3B1, which encodes 3b-HSD (hydroxysteroid dehydrogenase) responsible for androgen and progestagen biosynthesis from pregnenolone, was significantly overexpressed in AP-VEH animals relative to WO-VEH animals ($log_2$ [FC] = −2.98, FDR >0.001). Follow-up analyses via 2-way ANOVA of $log_{10}$ (cpm) expression levels of *HSD3B1* revealed significant effects of both site (p = 0.003; F (Diamanti-Kandarakis et al., 2009; Guillette et al., 1999) = 11.52) and FSH (p = 0.036; F (Diamanti-Kandarakis et al., 2009; Guillette et al., 1999) = 4.96; Fig. 4E), suggesting that elevated plasma androgens in both AP-VEH and AP-FSH animals relative to WO might be driven in part by increased activity of 3b-HSD in the ovary.

In contrast to estradiol and the three androgens described above, other steroid hormones were relatively homogenous across populations. Glucocorticoids, including, 11-deoxycorticosterone, 11-deoxycortisol, corticosterone, and cortisol, were detectable in plasma but did not differ across population or with FSH treatment. Progesterone and 17-hydroxyprogesterone were similarly equivalent across populations and with FSH, as was aldosterone (Figs. S1A–G (Hale and Parrott, 2022)). Androsterone, cortisone, DHEA, DHEA-S, DHT, and estrone were consistently below limits of detection.

### 3.4. Ovarian cellular responses to gonadotropin stimulation

We have previously reported significant reductions in the density of stage III oocytes in AP animals relative to WO, and that these differences are not rescued by FSH administration (Hale and Parrott, 2020). To further characterize population divergence in oocyte development and the effects of FSH, we quantified both the number and relative cellular density of germ cell beds, which contain PGCs, and stage I and stage II oocytes (Fig. 5C–F), as well as the relative proportions of total cortical area occupied by sIII oocytes or germ cell beds. Consistent with our previous findings that sIII oocyte density is lower in AP animals than WO, we observed a highly significant effect of population (p < 0.001; $F_{1, 23}$ = 31.58) on sIII follicle area, wherein the proportion of total cortical area occupied by sIII follicles (Fig. 5A) was greater in WO animals than AP. Post-hoc analyses confirmed this relationship within both VEH (adj. p < 0.001; predicted mean difference = −0.3402) and FSH (adj. p = 0.014; predicted mean difference = −0.221) groups individually. We observed a reciprocal increase in the proportion of cortical area occupied by germ cell beds (Fig. 5B) in AP ovaries. This increase was significant (p = 0.007; $F_{1,23}$ = 8.675) but post-hoc analyses did not reveal specific differences within FSH or VEH groups. This change was driven by increases in overall bed size but not bed number, as neither bed density (number of beds per unit area of ovarian cortex) (Fig. S2A (Hale and Parrott, 2022)) nor cell density within beds (Fig. S2B (Hale and Parrott, 2022)) differed between sites. Together, these observations highlight two distinct ovarian phenotypes between populations. At WO, the ovarian cortex is characterized by relatively small germ cell beds punctuated by connective trabeculae and numerous sIII follicles (Fig. 5C

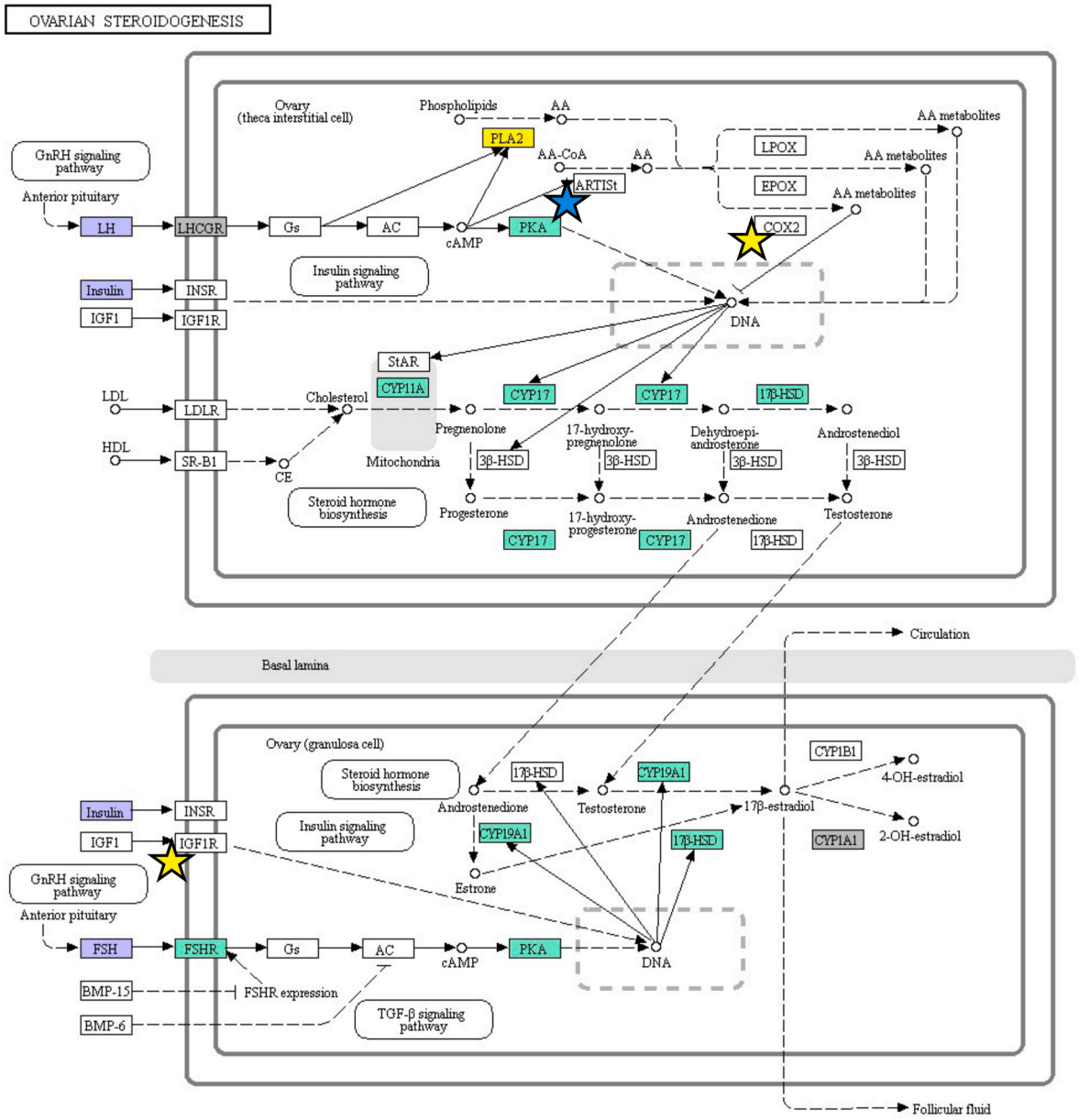


**Fig. 3. Divergent transcriptional responses in ovarian steroidogenesis components.** KEGG ovarian steroidogenesis pathway depicting expression patterns in FSH-challenged WO animals. Aquamarine boxed-terms correspond to genes significantly overexpressed in FSH-treated animals relative to VEH; yellow boxed terms correspond to genes expressed at significantly lower levels in FSH-treated animals; white terms are not significantly different between FSH and VEH groups. Grey terms were not detected and expression of purple terms was not assessed. Terms marked with stars represent a uniquely responsive gene detected at AP; yellow stars denote genes that were uniquely downregulated in FSH-treated AP animals relative to VEH while blue stars denote genes that were uniquely upregulated in FSH-treated AP animals relative to VEH. All genes expressed at WO were also expressed at AP and vice versa.

and D). This contrasts with the AP phenotype, wherein the cortex is occupied by large, uninterrupted beds and is only sparsely populated by late-stage sIII oocytes (Fig. 5E and F).

### 3.5. Gene expression network analysis and trait associations

Lastly, considering the broad transcriptomic differences observed between these two populations and concomitant divergence in steroidogenic and cellular phenotypes, we sought to delineate patterns of ovarian gene expression with respect to histological and steroidogenic traits. To this end, we employed a network-based approach to partitioning the ovarian transcriptome into clusters, or modules, of associated genes and then used principal components analysis to generate module eigengenes (principal component 1) as summarized expression profiles for each module. Eigengene expression profiles were then screened for associations with divergent traits (plasma androgen levels, germ cell bed), FSH stimulation (FSH, VEH), and population (AP, WO).

Network analysis with WGCNA yielded a transcriptional framework comprised of 12 modules of co-expressed genes that ranged in size from 6229 to 35 member genes and one orphan cluster of 562 non-associating genes. Module expression overall was strongly associated with trait population, FSH status, and androgen levels (testosterone, androstenedione, and etiocholanolone). Eigengenes for 11 of 12 modules were significantly associated with at least one trait, and 10 of 12 were associated with two traits or more (Table 1). Consistent with prior observations that site of origin (AP, WO) contributes strongly to transcription patterns in the ovary (Hale et al., 2019; Hale and Parrott, 2020), site was the strongest driver of co-expression patterns and was significantly

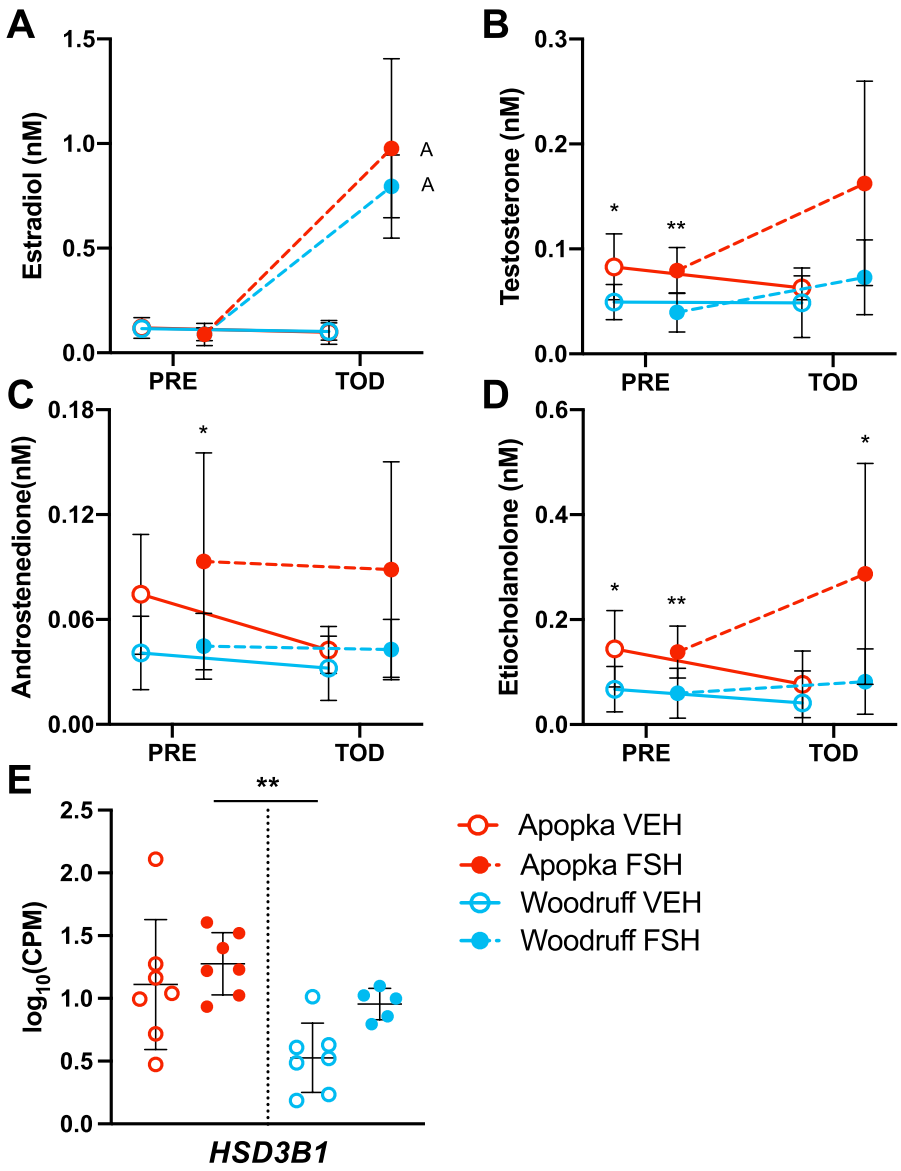


**Fig. 4. Steroidogenic Responses to Gonadotropin Treatment.** Plasma concentrations (nM) of steroid hormones estradiol (A), testosterone (B), androstenedione (C), and etiocholanolone (D) in WO (blue) and AP (red) animals treated with FSH (open circles, solid connecting lines) or vehicle control (VEH; closed circles, dashed connecting lines). Plasma levels were quantified at two time points for each treatment group, prior to the start of FSH challenge (PRE) and at its conclusion (TOD). Circles depict group means and error bars denote 1 SD. Letters to the right of group means designate significant differences detected in post-hoc analyses (Mann Whitney test) between PRE and TOD timepoints for a given treatment group. Asterisks above group means designate significant differences between groups detected in post-hoc analyses (Mann Whitney test) between WO and AP animals. (E) $Log_{10}$ transformed expression levels (counts per million; cpm) of HSD3B1 in FSH- and VEH-treated WO and AP animals. Bars depict group mean ± 1 SD. Asterisks above group mean denote a significant main effect of site on expression levels.

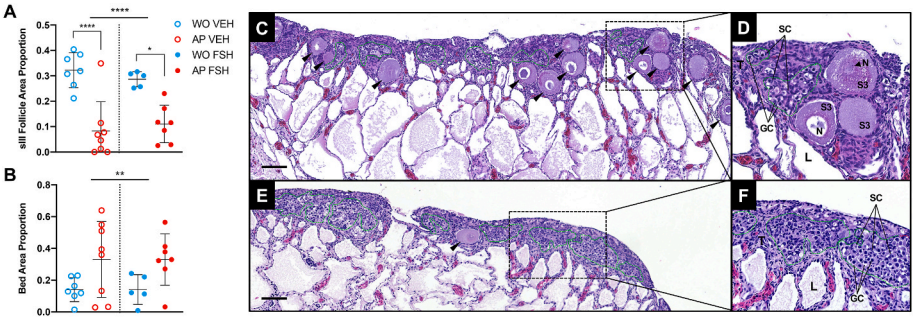


**Fig. 5. Ovarian follicle and germ cell dynamics across site and gonadotropin stimulation.** Total cortical area occupied by sIII follicles (A) and germ cell beds (B) are depicted in WO (blue) and AP (red) animals treated with either FSH (closed circles) or VEH (open circles). Bars depict group mean ± 1 SD. Asterisks above figures denote significant main effects of population while brackets with asterisks connecting specific groups denote significant group differences detected in post-hoc analyses (Sidak's multiple comparisons test). Representative images from VEH-treated WO (C, D inset) and AP (E, F inset) ovarian cross-sections depicting sIII follicles (S3; black arrows) and germ cell beds (green outlined regions). (D, F insets) SIII follicles contain distinctive large nuclei (N) with punctate nucleoli and a large basophilic ooplasm. Germ cell beds in contrast contain a larger number of smaller sI-sII follicles and germ cells. Germ cells and follicles (GC) within beds can be distinguished from somatic cells (SC) by their large, spherical nuclei, whereas somatic cell nuclei are ovoid and elongated. Connective tissue trabeculae (T) extend upwards from ovarian lacunae (L) and occur throughout the cortex, demarcating germ cell beds and sIII follicles. Ovarian sections are composite-stitched from multiple images per slide taken at 10× (E, F) or 20× (C, D). Scale bars = 100 μm.

**Table 1**
**WGCNA Module Summary**. Module number, size, hub gene, and associations with traits are reported, as well as the overlap of module genes with FSH-responsive DEGs in each population. Model effects summarize results from linear models – arrows denote the direction of effect and p-values.

| Module Summary | | | | Model Effects | | | | | | DEG Module Membership | | | |
|---|---|---|---|---|---|---|---|---|---|---|---|---|---|
| Module | Color | Module Genes | Hub Gene | Site | FSH | Bed Area Proportion | Testosterone | Androstenedione | Etiocholanolone | WO FSH Up | WO FSH Down | AP FSH Up | AP FSH Down |
| 0 | Grey | 562 | – | – | – | – | – | – | – | 2 | 1 | 0 | 34 |
| 1 | Turquoise | 6229 | THAP4 | **WO > AP (<0.001)** | – | **↓ (0.002)** | – | ↓ (0.083) | – | 0 | 102 | 5 | 623 |
| 2 | Blue | 3240 | ACADS | **AP > WO (<0.001)** | – | **↑ (0.020)** | – | – | – | 404 | 0 | 42 | 1 |
| 3 | Brown | 2789 | LOC106739643; PACS2-like | **AP > WO (<0.001)** | **↓ (0.002)** | **↑ (0.022)** | – | – | – | 2 | 84 | 0 | 1405 |
| 4 | Yellow | 1928 | CHCHD3 | **AP > WO (0.003)** | **↑ (<0.001)** | **↑ (<0.001)** | **↑ (0.047)** | **↑ (0.012)** | ↑ (0.077) | 1317 | 0 | 1495 | 0 |
| 5 | Green | 1328 | GTF2E1 | **WO > AP (<0.001)** | – | – | – | – | – | 3 | 0 | 750 | 0 |
| 6 | Red | 973 | DNAAF1 | **AP > WO (<0.001)** | – | **↑ (0.010)** | – | – | – | 1 | 0 | 0 | 647 |
| 7 | Black | 609 | HYOU1 | **AP > WO (0.027)** | **↑ (<0.001)** | – | **↑ (0.036)** | **↑ (0.019)** | **↑ (0.046)** | 231 | 0 | 536 | 0 |
| 8 | Pink | 326 | PIK3IP1 | WO > AP (0.067) | **↓ (<0.001)** | – | **↓ (0.006)** | **↓ (0.004)** | **↓ (0.025)** | 0 | 60 | 0 | 313 |
| 9 | Magenta | 242 | LOC102565488; TUBA3C | – | **↓ (0.011)** | ↑ (0.098) | – | ↓ (0.083) | **↓ (0.044)** | 0 | 1 | 0 | 175 |
| 10 | Purple | 128 | LCP1 | – | – | – | – | – | – | 5 | 0 | 0 | 9 |
| 11 | Green yellow | 46 | TH | AP > WO (0.068) | – | – | ↓ (0.088) | – | – | 0 | 0 | 0 | 1 |
| 12 | Tan | 35 | LOC102559263; HBB | – | – | **↑ (0.043)** | – | – | – | 0 | 0 | 0 | 0 |
| | | | | | | | | | ***DEGS in list*** | 1965 | 248 | 2828 | 3208 |

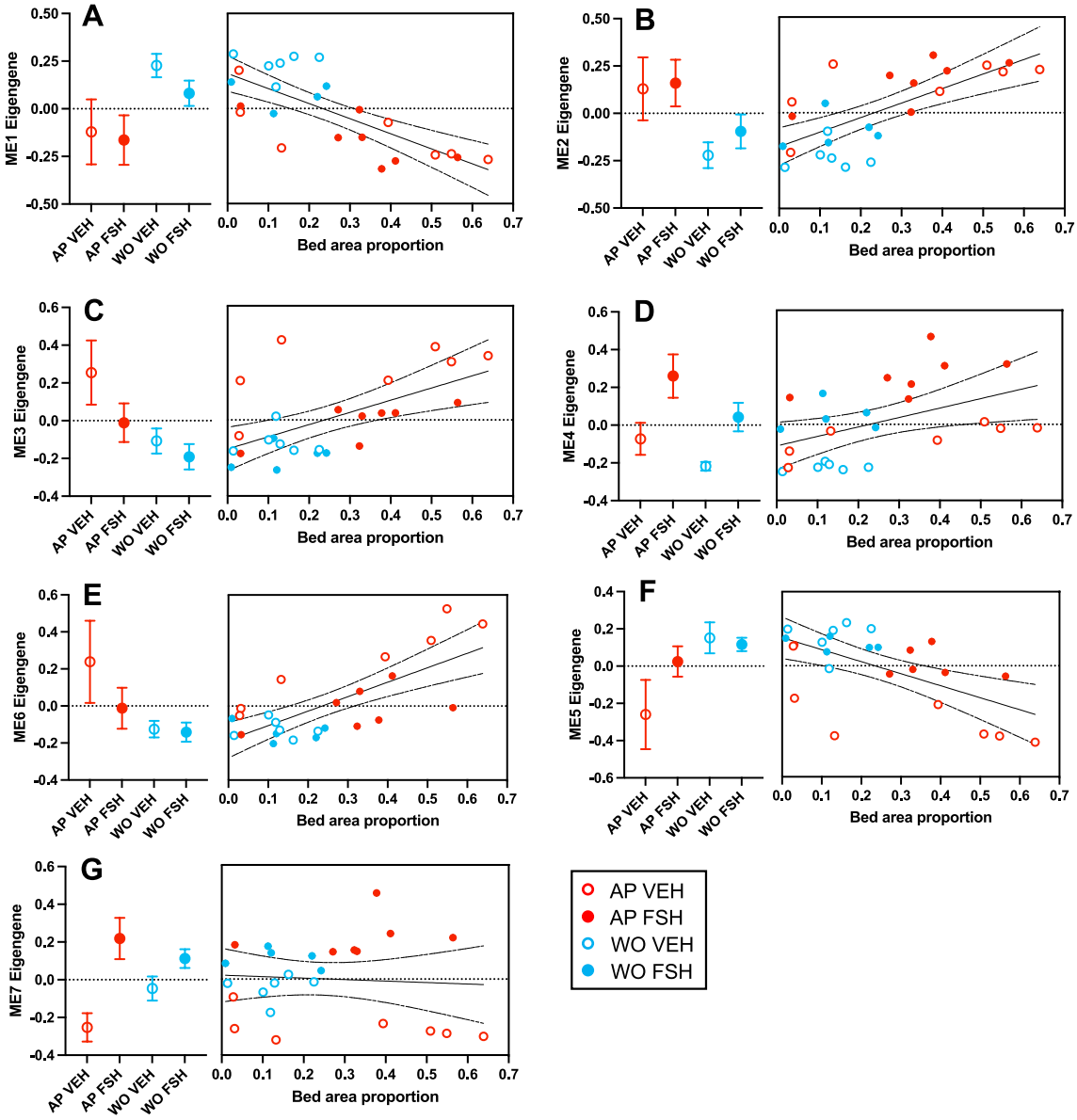


**Fig. 6. Site-associated module eigengenes**. The relationship between eigengenes and bed area proportion is depicted for 7 significant site-associated modules. Five modules (A–E) exhibited concomitant significant associations with bed area proportion while two cell-autonomous modules were observed (F, G). Circles in leftmost graphs depict group mean ± 1 SD for AP (red) and WO (blue) animals treated with FSH (closed circles) or VEH (open circles). Circles on scatter plots denote eigengene values for individual samples; solid lines depict lines of best fit from simple linear regressions ±95% confidence interval.

associated with 7 module eigengenes, and with two additional module eigengenes that approached significance ($0.05 < p < 0.10$). We also observed persistent effects of bed area proportion (6 of 12 modules + 1 module approaching significance) and gonadotropin stimulation (5 of 12 modules) on network structure. Lastly, 4 of 12 modules were significantly associated with at least one androgen hormone (+2 additional modules approaching significance).

### 3.6. *Module-phenotype associations, functional enrichment, and hub genes*

To identify specific phenotypic drivers of network structure and transcriptomic divergence between AP and WO, we next sought to identify patterns of module eigengene co-association within the cohort of site-associated modules. Nearly all site-associated modules were also significantly associated with either bed area proportion or one of the three hormones surveyed, but the majority (5 of 7) were associated with bed area proportion (Fig. 6A–E). This subset of 5 modules collectively represented a large proportion of the ovarian transcriptome (15,159 of 18,435 total expressed genes; 82.2%), indicating that the expression levels of most genes covary with the cellular composition of the ovary. In contrast, a relatively small pair of site-associated modules was observed to display no significant associations with bed area proportion (1937 of 18,435; 10.5%) and thus likely contain genes for which expression diverges in a cell-autonomous manner (Fig. 6F and G).

All five site- and bed-associated modules were enriched for distinct biological functions (Gene Ontology: Biological Process) and module hub genes, which represent the most highly connected or central genes to a given module (Langfelder and Horvath, 2008), frequently mirrored these functions. The largest module M1, was significantly enriched for genes related to transcription and cell process (Fig. 7, "Turquoise_g-Profiler.xlsx") and its hub gene THAP domain containing 4 (THAP4),

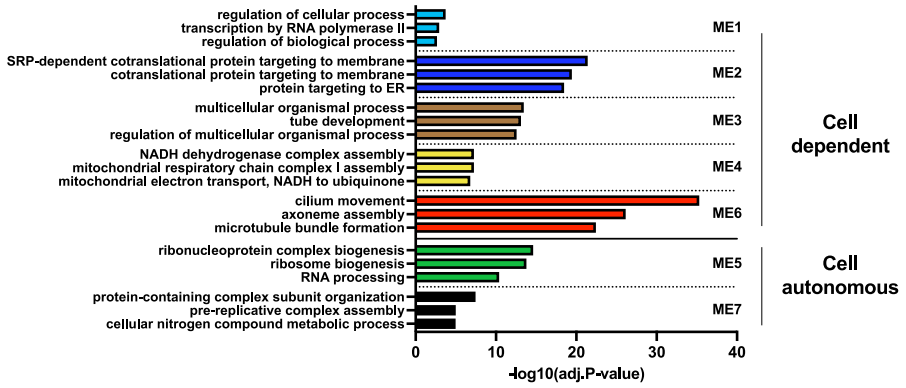


**Fig. 7. Module member gene pathway enrichment**. Top 3 functional pathways (GO: biological process) significantly enriched in member genes of site-associated modules where significant relationships were or were not detected with bed-area proportion (cell dependent and cell autonomous, respectively). Colors correspond to module colors assigned during network construction (Table 1).

possesses a zinc-finger DNA binding domain shared with other THAP domain proteins that regulate transcription, cell proliferation, and apoptosis (Cayrol et al., 2007; Macfarlan et al., 2005; Seifert et al., 2017). Module 2 was highly enriched for translational pathways and protein targeting to the endoplasmic reticulum ("Blue_gProfiler.xlsx") while its hub gene, acyl-CoA dehydrogenase short chain (ACADS), regulates mitochondrial fatty acid metabolism to acetyl-CoA. M3 in contrast was enriched for a relatively large term, multicellular organismal process, but subordinate enriched terms were identified related to tube formation and vascular development ("Brown_gProfiler.xlsx"). M3 hub gene, LOC106739643, or phosphofurin acidic cluster sorting protein 2-like (PACS2-like), putatively regulates apoptosis and membrane trafficking (Li et al., 2020). ME4 was almost exclusively enriched for pathways related to mitochdondrial respiratory function ("Yellow_gProfiler.xlsx"). Consistent with this function, M4 hub gene coiled-coil-helix-coiled-coil-helix domain containing 3 (CHCHD3) encodes a mitochondrial scaffold protein integral to cristae morphology and overall mitochondrial function (Darshi et al., 2011). The last site-associated module, module 6 was highly enriched for pathways relating to cilium movement and assembly ("Red_gProfiler.xlsx") and its hub gene, DNAAF1, is an integral ciliary component (Van Rooijen et al., 2008).

The two site-associated modules that lacked significant associations with bed area proportion, M5 (Fig. 6F) and M7 (Fig. 6G), were also enriched for specific biological functions (Fig. 7). Genes related to ribosome biogenesis and RNA processing were overrepresented in module 5 in addition to mitotic and cell cycle pathways ("Green_gProfiler.xlsx"). Its hub gene was general transcription factor IIE (GTF2E1). Finally, module 7 was significantly enriched for pathways related to protein complex organization, including pre-replicative complex assembly and nitrogen compound metabolism. In addition to these top enriched terms, however, other pathways were found relating to posttranscriptional mRNA modification, splicing, and translation ("Black_gProfiler.xlsx"). Its hub gene, hypoxia upregulated 1 (HYOU1), belongs to the Hsp70 family of protein chaperones and itself regulates protein folding and degradation in the endoplasmic reticulum (Inoue

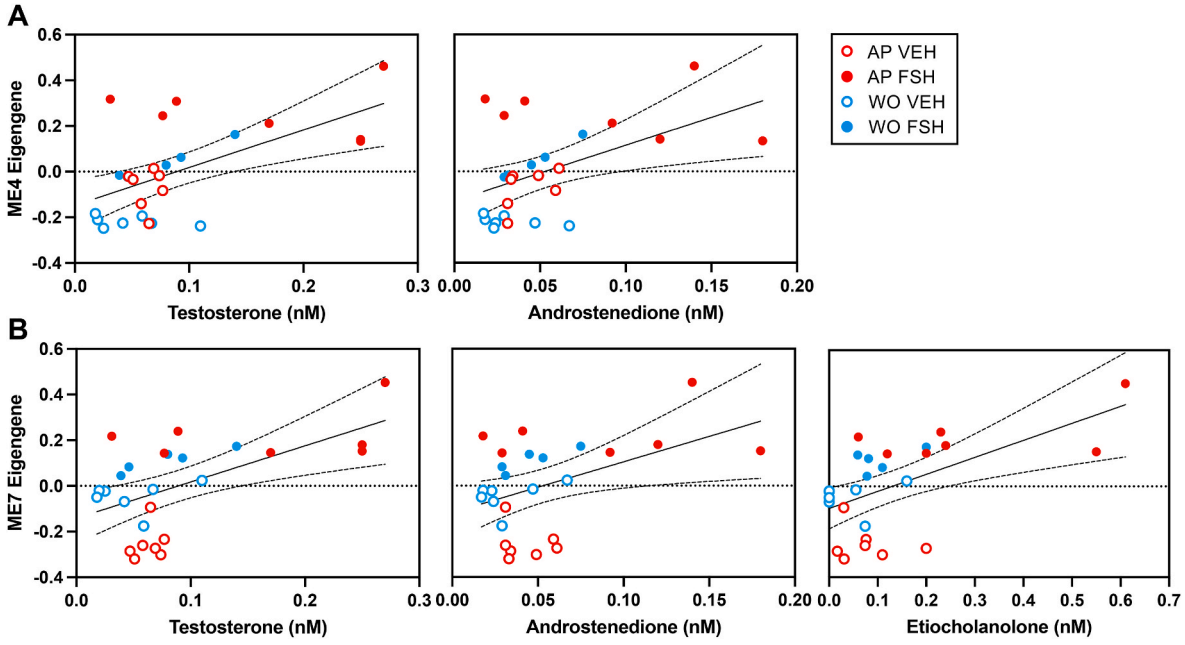


**Fig. 8. Androgen-associated module eigengenes.** The relationship between concentrations of testosterone and androstenedione (A) or testosterone, androstenedione, and etiocholanolone (B) is depicted for two site-associated modules. Circles on scatter plots denote eigengene values for individual samples: AP VEH (red, open circles), AP FSH (red, closed circles), WO VEH (blue, open circles), WO FSH (blue, closed circles). Solid lines depict lines of best fit from simple linear regressions ±95% confidence interval.

and Tsai, 2016).

### 3.7. Plasma androgens and site-associated modules

Associations between co-expression modules and any of the three androgen hormones were restricted to two site-associated modules, one cell-dependent module and one cell-autonomous module. ME4 was positively related to circulating levels of both testosterone and androstenedione, while a relationship with etiocholanolone only approached significance (Fig. 8A; etiocholanolone not shown). In contrast, ME7 was positively associated with all three hormones assayed (Fig. 8B). As M7 was the only site and hormone-associated module detected that displayed no detectable relationship with bed area proportion, it likely comprises a subset of genes with cell-autonomous divergent expression between WO and AP that is linked to levels of circulating androgens.

### 3.8. Gonadotropin stimulation

Three site-associated modules displayed significant relationships to gonadotropin stimulation, ME3 (Fig. 6C) ME4 (Fig. 6D), and ME7 (Fig. 6G; Table 1). ME3 alone was negatively associated with gonadotropin stimulation, decreasing in FSH-treated groups relative to VEH animals. In contrast, ME4 and ME6 contained genes positively associated with FSH stimulation. Despite only three modules detected as significantly associated with FSH status, we observed that all site-associated modules contained FSH-responsive DEGs. Furthermore, the direction of response to FSH (upregulated or downregulated) for these DEGs was reflected in site-specific changes to module eigengenes. ME1 (Fig. 6A) contained 102 of 248 total (41.1%) of genes downregulated by FSH in WO animals (Table 1), concomitant with a reduction in eigengene values in WO animals (VEH vs FSH) that was less apparent in AP animals. Consequently, ME1 contained a much smaller proportion (19.4%) of DEGs downregulated with FSH treatment in AP animals. This pattern was also observed for ME2, which contained a greater proportion of DEGs upregulated by FSH in WO animals (20.6%) relative to DEGs upregulated in AP animals (1.48%). Lastly, ME5 displayed the inverse relationship between site and FSH-responsive DEGs; ME5 contained 26.5% of DEGs upregulated in AP animals but only 0.15% of WO upregulated DEGs. Summarily, ME5 eigengene values appeared to be positively associated with FSH in AP animals but not WO.

## 4. Discussion

In the current study, we report stark differences in transcriptional, endocrine, and histological responses to gonadotropin signaling in alligators originating from two neigboring lakes (separated by only 48 km) that confer disparate exposures to EDCs. Whereas previous studies of these populations have identified reproductive perturbations consistent with those reported here, they typically assessed gene expression, estrogen and testosterone levels, and ovarian histology independent of one another and relied on targeted methodology (e.g., candidate approaches). When these traits are broadly assessed and viewed collectively within the same individuals, a clearer view of the "Apopka phenotype" emerges in which the interlinkages between hyperandrogenism, impaired follicle maturation, and ovarian transcriptional dysregulation yield a reproductive disorder which mirrors aspects of human infertility. For example, a partial or complete reduction in the number of maturing follicles is a fundamental characteristic of primary ovarian insufficiency (POI), which affects 1–2% of women globally (Wesevich et al., 2020; Chon et al., 2021). Due to the multifaceted etiology and idiopathic nature of POI, the underlying mechanisms are likely to involve a multitude of genetic and endocrine pathways (Jiao et al., 2018; Richardson et al., 2014). However, similar to ovaries of AP alligators, primordial and primary follicles are observed in a substantial proportion of cases, and arrested folliculogenesis, rather than a general lack of germinal precursors, is likely a key driver (Wesevich et al., 2020; Massin et al., 2004; Pastore et al., 2018).

Patients with POI are also generally unresponsive to gonadrotropin treatment (Wesevich et al., 2020; Massin et al., 2004; Pastore et al., 2018). Despite eliciting robust transcriptional responses in ovaries of AP alligators, FSH stimulation does not result in follicular growth, suggesting that folliculogenesis itself is impeded rather than a general insensitivity of the ovary to gonadotropin signaling. Whether these observations reflect alterations to the FSH-mediated transcriptional program or follicle arrests occurring prior to gonadotropin-dependent growth is not clear, but additional experiments aimed at elucidating the events that precipitate observed blockades in follicle development have the potential to reveal the environmental determinants of reproductive health both in wildlife as well as humans. Despite parallels to human POI, care should be taken when interpreting findings in juvenile alligators, as it is unclear to what extent adult alligators inhabiting AP display reductions in mature follicles and their attendant response to gonadotropin signaling remains uncharacterized. Patients with POI typically have decreased levels of circulating estrogen and elevated levels of FSH (Wesevich et al., 2020; Chon et al., 2021; Ferraretti et al., 2011). Whereas elevated estrogen levels have been reported in juvenile female alligators from AP (Guillette et al., 1994), estrogen and FSH levels have yet to be assayed in adults.

Previous work with this dataset uncovered considerable overlap in ovarian transcriptional and cellular abnormalities between AP alligators and WO alligators dosed with estradiol during embryonic development (Hale and Parrott, 2020). Taking together with our findings herein, this suggests that the cocktail of EDCs at AP acts via an estrogenic mode of action to disrupt gonadotropin-regulated transcriptional networks in the ovary and follicular development. This is perhaps unsurprising considering that many organochlorine pesticides documented in alligator egg yolk at AP can activate the estrogen receptor *in vitro*, including *p,p'*-DDE, *trans*-nonachlor, toxaphene, and dieldrin (Soto et al., 1994; Vonier et al., 1996; Klotz et al., 1996). Interestingly, however, embryonic dosing studies in alligators using individual contaminants in isolation have largely failed to recapitulate aspects of the AP phenotype (Milnes et al., 2004, 2005). This would suggest that abnormalities observed herein are driven in part by synergistic effects of contaminant mixtures (Kortenkamp, 2007a, 2007b).

Most of the coexpression modules identified in the current study were associated with the proportion of ovarian cortex occupied by germ cell beds. This finding indicates that expression patterns for much of the ovarian transcriptome covaries with cellular architecture, an observation that is consistent with prior findings that much of the ovarian transcriptome is correlated with the density of stage III follicles (Hale and Parrott, 2020). Among all site-associated modules, module 1 captured over a third of all expressed ovarian genes (6229 of 18435) that were expressed at lower levels in AP animals relative to WO and were concomitantly negatively associated with increasing bed area proportion. Further, previous analysis using this dataset revealed that DEGs suppressed at AP were functionally enriched for cell cycle and replication pathways (Hale and Parrott, 2020). However, the underlying cause (s) of disrupted ovarian morphology at AP have yet to be fully resolved as delineating direct, organizational effects resulting from *in ovo* contaminant exposure from contemporary manifestations of *in ovo* exposures (e.g., elevated androgen levels) remains challenging. As such, identification of THAP4 as the hub gene of a large module associated with both site and follicle development sheds light on novel, putative mechanisms underlying the AP phenotype by linking altered ovarian cellular architecture to the expression of a transcriptional regulator of cell-proliferation and differentiation. Although the functions of THAP4 have not been well characterized and its role, if any, in the ovary remains undescribed, it possesses the characteristic THAP domain, a zinc-finger DNA binding domain with broad evolutionary conservation across animals (Roussigne et al., 2003; Clouaire et al., 2005). Other THAP-containing proteins have been found to regulate transcription, replication, and proliferation. This includes THAP1, THAP5, and

THAP7, which regulate DNA synthesis and cell proliferation by dictating expression of cell-cycle regulators, such as p21 and targets of pRb/E2F signaling (Cayrol et al., 2007; Chen et al., 2019; Balakrishnan et al., 2009). In contrast, THAP11 (Ronin), regulates DNA repair and differentiation in proliferative stem cell populations, and its loss is associated with stalled cell-cycle progression, while ectopic expression inhibits differentiation and maintains stemness in ESCs (Seifert et al., 2017; Dejosez et al., 2008). In our DEG analyses, THAP4 as well as THAP1, 3, 6, 7, 11, and 12 were all significantly suppressed in AP animals. Thus, future work in this system should aim to 1.) characterize distinct functional roles for THAP proteins in the ovary, 2.) identify putative transcriptional targets among dysregulated genes at AP, and 3.) uncover how contaminant exposures early in development might manifest as contemporary alterations to THAP expression.

Previous studies have identified persistent effects of developmental contaminant exposure on transcriptional responses to gonadotropins within the alligator ovary. These studies, primarily incorporating targeted, candidate gene approaches, consistently report abated transcriptional responses in AP animals, including suppression of both basal and FSH-induced expression of follistatin, inhibins, FSHR, CYP19A1, and nuclear transcription factors/hormone receptors (Moore et al., 2010c, 2012a, 2012b; Hale et al., 2019). This pattern is recapitulated to some degree by our observations herein; although both WO and AP animals respond to FSH by significantly upregulating CYP19A1 and FST, $\log_2$(FC) values are marginally higher between VEH and FSH groups at WO than AP (Fig. 2A). However, in contrast to these previous reports, we observed the opposite pattern at the transcriptome level. Across all 18,435 expressed genes, median fold change values were higher between VEH and FSH treated animals from AP than WO (Fig. 2B). Furthermore, a substantially larger degree of DEGs were detected, including novel genes stimulated and suppressed by FSH at AP relative to WO. Thus, while core FSH responses are conserved in both populations (Fig. 3), the AP phenotype encompasses both more significantly responsive genes overall (DEGs) and a net higher measure of responsiveness at the transcriptome level ($\log_2$ [FC]). Our findings, when interpreted along with prior studies, suggest that altered transcriptional responses to gonadotropin signaling in Lake Apopka alligators are not due to a general insensitivity to gonadotropin signaling (e.g., resulting from suppressed ovarian expression of the FSH receptor), but instead represent a largely distinct and highly complex response likely resulting from both organizational changes to the underlying ovarian cellular architecture as well as disrupted epigenetic patterning.

The findings reported here collectively advance our mechanistic understanding of interactions between the vertebrate endocrine system and environmental contaminants in a well-established model of endocrine disruption. Historically, studies of perturbed reproductive function in Lake Apopka alligators and other non-traditional models pioneered our understanding of the ecological consequences and broad scope by which EDCs are impacting our world. The question of whether EDC exposure is detrimental to reproductive health is no longer debated, but instead the field now grapples with resolving how exposures to endless and everchanging combinations of legacy and emerging contaminants occurring across a lifespan interact with other environmental stressors and genomic influences to ultimately determine health outcomes in individuals, populations, and even ecosystems. Reductionist approaches have established causality, but to meet the current challenges, integrative studies incorporating a broad range of taxonomic diversity and embracing the complexity inherent to the natural world are now clearly needed.

## Disclosure summary

The authors have no conflicts of interest to disclose.

## Data availability

Original data generated and analyzed during this study are included in this published article or in the data repositories listed in References.

## Acknowledgements

The authors would like to thank Russell Lowers, Arnold Brunell, and colleagues at the Florida Fish and Wildlife Conservation Commission for their assistance with permitting and egg collections. We would also like to thank Shane Campbell-Staton, Doug Menke, and member of the Parrott and Guillette Laboratories for helpful conversations, assistance in animal husbandry, and access to instrumentation. This work was supported by the National Science Foundation (Award #1754903 to BBP) and the Department of Energy National Nuclear Security Administration under award number DE-EM0004391. This report was prepared as an account of work sponsored by an angency of the United States Government. The views and opinions of authors expressed herein do not necessarily state or reflect those of the United States Government or any agency thereof.

## Appendix A. Supplementary data

Supplementary data to this article can be found online at https://doi.org/10.1016/j.mce.2022.111751.

## References

Alviggi, C., Conforti, A., Esteves, S.C., Vallone, R., Venturella, R., Staiano, S., Castaldo, E., Andersen, C.Y., De Placido, G., 2018. Understanding ovarian hyporesponse to exogenous gonadotropin in ovarian stimulation and its new proposed marker-the follicle-to-oocyte (FOI) index. Front. Endocrinol. 9 (OCT) https://doi.org/10.3389/fendo.2018.00589.

Apweiler, R., Bairoch, A., Wu, C.H., Barker, W.C., Boeckmann, B., Ferro, S., Gasteiger, E., Huang, H., Lopez, R., Magrane, M., Martin, M.J., Natale, D.A., O'Donovan, C., Redaschi, N., Yeh, L.S.L., 2004. UniProt: the universal protein knowledgebase. Nucleic Acids Res. 32 https://doi.org/10.1093/nar/gky092 (DATABASE ISS.).

Bae, J., Bertucci, E.M., Bock, S.L., Hale, M.D., Moore, J., Wilkinson, P.M., Rainwater, T. R., Bowden, J.A., Koal, T., PhamTuan, H., Parrott, B.B., 2021. Intrinsic and extrinsic factors interact during development to influence telomere length in a long-lived reptile. Mol. Ecol. https://doi.org/10.1111/mec.16017.

Balakrishnan, M.P., Cilenti, L., Mashak, Z., Popat, P., Alnemri, E.S., Zervos, A.S., 2009. THAP5 is a human cardiac-specific inhibitor of cell cycle that is cleaved by the proapoptotic Omi/HtrA2 protease during cell death. Am. J. Physiol. Heart Circ. Physiol. 297 (2) https://doi.org/10.1152/ajpheart.00234.2009.

Bloom, M.S., Fujimoto, V.Y., Storm, R., Zhang, L., Butts, C.D., Sollohub, D., Jansing, R.L., 2017. Persistent organic pollutants (POPs) in human follicular fluid and in vitro fertilization outcomes, a pilot study. Reprod. Toxicol. 67 https://doi.org/10.1016/j.reprotox.2017.01.004.

Cayrol, C., Lacroix, C., Mathe, C., Ecochard, V., Ceribelli, M., Loreau, E., Lazar, V., Dessen, P., Mantovani, R., Aguilar, L., Girard, J.P., 2007. The THAP-zinc finger protein THAP1 regulates endothelial cell proliferation through modulation of pRB/E2F cell-cycle target genes. Blood 109 (2). https://doi.org/10.1182/blood-2006-03-012013.

Chen, E.Y., Tan, C.M., Kou, Y., Duan, Q., Wang, Z., Meirelles, G.V., Clark, N.R., Ma'ayan, A., 2013. Enrichr: interactive and collaborative HTML5 gene list enrichment analysis tool. BMC Bioinf. 14 https://doi.org/10.1186/1471-2105-14-128.

Chen, Y., Lun, A.T.L., Smyth, G.K., 2016. From reads to genes to pathways: differential expression analysis of RNA-Seq experiments using Rsubread and the edgeR quasi-likelihood pipeline. F1000Research 5. https://doi.org/10.12688/F1000RESEARCH.8987.2.

Chen, C.P., Sang, Y., Liu, L., Feng, Z.Q., Liang, Z., Pei, X., 2019. THAP7 promotes cell proliferation by regulating the G1/S phase transition via epigenetically silencing p21 in lung adenocarcinoma. OncoTargets Ther. 12 https://doi.org/10.2147/OTT.S208908.

Chon, S.J., Umair, Z., Yoon, M.S., 2021. Premature ovarian insufficiency: past, present, and future. Front. Cell Dev. Biol. 9 https://doi.org/10.3389/fcell.2021.672890.

Clouaire, T., Roussigne, M., Ecochard, V., Mathe, C., Amalric, F., Girard, J.P., 2005. The THAP domain of THAP1 is a large C2CH module with zinc-dependent sequence-specific DNA-binding activity. Proc. Natl. Acad. Sci. U. S. A 102 (19). https://doi.org/10.1073/pnas.0406882102.

Colborn, T., Thayer, K., 2000. Aquatic ecosystems: harbingers of endocrine disruption. Ecol. Appl. 10 (4) https://doi.org/10.1890/1051-0761(2000)010[0949:AEHOED]2.0.CO;2.

Darshi, M., Mendiola, V.L., Mackey, M.R., Murphy, A.N., Koller, A., Perkins, G.A., Ellisman, M.H., Taylor, S.S., 2011. ChChd3, an inner mitochondrial membrane protein, is essential for maintaining Crista integrity and mitochondrial function. J. Biol. Chem. 286 (4) https://doi.org/10.1074/jbc.M110.171975.

Dejosez, M., Krumenacker, J.S., Zitur, L.J., Passeri, M., Chu, L.F., Songyang, Z., Thomson, J.A., Zwaka, T.P., 2008. Ronin is essential for embryogenesis and the pluripotency of mouse embryonic stem cells. Cell 133 (7). https://doi.org/10.1016/j.cell.2008.05.047.

Diamanti-Kandarakis, E., Bourguignon, J.P., Giudice, L.C., Hauser, R., Prins, G.S., Soto, A.M., Zoeller, R.T., Gore, A.C., 2009. Endocrine-disrupting chemicals: an endocrine society scientific statement. Endocr. Rev. 30 (4), 293–342.

Encarnação, T., Pais, A.A.C.C., Campos, M.G., Burrows, H.D., 2019. Endocrine disrupting chemicals: impact on human health, wildlife and the environment. Sci. Prog. 102 (1) https://doi.org/10.1177/0036850419826802.

Ewels, P., Magnusson, M., Lundin, S., Käller, M., 2016. MultiQC: summarize analysis results for multiple tools and samples in a single report. Bioinformatics 32 (19). https://doi.org/10.1093/bioinformatics/btw354.

Ferguson, M.W.J., 1985. Reproductive biology and embryology of the crocodilians. In: Billet, Gans F., Maderson, P.C. (Eds.), Biology of the Reptilia, vol. 14. J. Wiley and Sons, New York, pp. 329–491.

Ferraretti, A.P., La Marca, A., Fauser, B.C.J.M., Tarlatzis, B., Nargund, G., Gianaroli, L., 2011. ESHRE consensus on the definition of 'poor response to ovarian stimulation for in vitro fertilization: the Bologna criteria. Hum. Reprod. 26 (7) https://doi.org/10.1093/humrep/der092.

Forbes, T.R., 1939. Studies on the reproductive system of the alligator. V. The effects of injections of testosterone proprionate in immature alligators. Anat. Rec. 75, 51–57.

Galligan, T.M., Hale, M.D., McCoy, J.A., Bermudez, D.S., Guillette, L.J., Parrott, B.B., 2019. Assessing impacts of precocious steroid exposure on thyroid physiology and gene expression patterns in the American alligator (Alligator mississippiensis). Gen. Comp. Endocrinol. 271 https://doi.org/10.1016/j.ygcen.2018.11.002.

Guillette, L.J.J., 1994. Developmental Abnormalities of the Reproductive System of Alligators (Alligator mississippiensis) from Contaminated and Control Lakes in Florida. Hearing on: "Health Effects of Estrogenic Pesticides". Subcommittee on Health and the Environment. Congressman Henry A. Waxman, Chairman.

Guillette Jr., L.J., Gunderson, M.P., 2001. Alterations in the development of the reproductive and endocrine systems of wildlife exposed to endocrine disrupting contaminants. Reproduction 122, 857–864.

Guillette, L.J., Gross, T.S., Masson, G.R., Matter, J.M., Percival, H.F., Woodward, A.R., 1994. Developmental abnormalities of the gonad and abnormal sex hormone concentrations in juvenile alligators from contaminated and control lakes in Florida. Environ. Health Perspect. 102 (8), 680–688.

Guillette Jr., L.J., Brock, J.W., Rooney, A.A., Woodward, A.R., 1999. Serum concentrations of various environmental contaminants and their relationship to sex steroid concentrations in juvenile American alligators. Arch. Environ. Contam. Toxicol. 36, 447–455.

Hale, M.D., Parrott, B.B., 2020. Assessing the ability of developmentally precocious estrogen signaling to recapitulate ovarian transcriptomes and follicle dynamics in alligators from a contaminated lake. Environ. Health Perspect. https://doi.org/10.1289/EHP6627.

Hale, M.D., Parrott, B.B., 2022. Supplementary data in dryad repository. https://doi.org/10.5061/dryad.0rxwdbs33.

Hale, M.D., McCoy, J.A., Doheny, B.M., Galligan, T.M., Guillette, L.J., Parrott, B.B., 2019. Embryonic estrogen exposure recapitulates persistent ovarian transcriptional programs in a model of environmental endocrine disruption. Biol. Reprod. 100 (1) https://doi.org/10.1093/biolre/ioy165.

Heinz, G.H., Percival, H.F., Jennings, M.L., 1991. Contaminants in American alligator eggs from lakes Apopka, griffin and okeechobee, Florida. Environ. Monit. Assess. 16, 277–285.

Inoue, T., Tsai, B., 2016. The Grp170 nucleotide exchange factor executes a key role during ERAD of cellular misfolded clients. Mol. Biol. Cell 27 (10). https://doi.org/10.1091/mbc.E16-01-0033.

Jiao, X., Ke, H., Qin, Y., Chen, Z.J., 2018. Molecular genetics of premature ovarian insufficiency. Trends Endocrinol. Metabol. 29 (11) https://doi.org/10.1016/j.tem.2018.07.002.

Kahn, L.G., Philippat, C., Nakayama, S.F., Slama, R., Trasande, L., 2020. Endocrine-disrupting chemicals: implications for human health. Lancet Diabetes Endocrinol. 8 (8) https://doi.org/10.1016/S2213-8587(20)30129-7.

Kim, D., Langmead, B., Salzberg, S.L., 2015. HISAT: a fast spliced aligner with low memory requirements. Nat. Methods 12 (4). https://doi.org/10.1038/nmeth.3317.

Klotz, D.M., Beckman, B.S., Hill, S.M., Mclachlan, J.A., Walters, R., Arnold, S.F., 1996. Identification of environmental chemicals with estrogenic activity using a combination of in vitro. Environ. Health Perspect. 104 (10), 1084–1089.

Koal, T., Schmiederer, D., Pham-Tuan, H., Röhring, C., Rauh, M., 2012. Standardized LC-MS/MS based steroid hormone profile-analysis. J. Steroid Biochem. Mol. Biol. 129 (3–5), 129–138.

Kortenkamp, A., 2007a. Introduction: endocrine disruptors-exposure assessment, novel end points, and low-dose and mixture effects. Environ. Health Perspect. 115 (Suppl. 1) https://doi.org/10.1289/ehp.10517.

Kortenkamp, A., 2007b. Ten years of mixing cocktails: a review of combination effects of endocrine-disrupting chemicals. Environ. Health Perspect. 115 (Suppl. 1) https://doi.org/10.1289/ehp.9357.

Kuleshov, M.V., Jones, M.R., Rouillard, A.D., Fernandez, N.F., Duan, Q., Wang, Z., Koplev, S., Jenkins, S.L., Jagodnik, K.M., Lachmann, A., McDermott, M.G., Monteiro, C.D., Gundersen, G.W., Maayan, A., 2016. Enrichr: a comprehensive gene set enrichment analysis web server 2016 update. Nucleic Acids Res. 44 (1) https://doi.org/10.1093/nar/gkw377.

Langfelder, P., Horvath, S., 2008. WGCNA: an R package for weighted correlation network analysis. BMC Bioinf. 9 https://doi.org/10.1186/1471-2105-9-559.

Lawrence, M., Huber, W., Pagès, H., Aboyoun, P., Carlson, M., Gentleman, R., Morgan, M.T., Carey, V.J., 2013. Software for computing and annotating genomic ranges. PLoS Comput. Biol. 9 (8), 1–10.

Li, C., Li, L., Yang, M., Zeng, L., Sun, L., 2020. PACS-2: a key regulator of mitochondria-associated membranes (MAMs). Pharmacol. Res. 160. https://doi.org/10.1016/j.phrs.2020.105080.

Love, M., Huber, W., Anders, S., 2014. Moderated estimation of fold change and dispersion for RNA-seq data with DESeq2. Genome Biol. 15, 550.

Love, M., Anders, S., Huber, W., 2017. Analyzing RNA-Seq Data with DESeq2, vol. 2. Bioconductor (January).

Macfarlan, T., Kutney, S., Altman, B., Montross, R., Yu, J., Chakravarti, D., 2005. Human THAP7 is a chromatin-associated, histone tail-binding protein that represses transcription via recruitment of HDAC3 and nuclear hormone receptor corepressor. J. Biol. Chem. 280 (8) https://doi.org/10.1074/jbc.M411675200.

Mahalingaiah, S., Missmer, S.A., Maity, A., Williams, P.L., Meeker, J.D., Berry, K., Ehrlich, S., Perry, M.J., Cramer, D.W., Hauser, R., 2012. Association of hexachlorobenzene (HCB), dichlorodiphenyltrichloroethane (DDT), and Dichlorodiphenyldichloroethylene (DDE) with in vitro fertilization (IVF) outcomes. Environ. Health Perspect. 120 (2) https://doi.org/10.1289/ehp.1103696.

Massin, N., Gougeon, A., Meduri, G., Thibaud, E., Laborde, K., Matuchansky, C., Constancis, E., Vacher-Lavenu, M.C., Paniel, B., Zorn, J.R., Misrahi, M., Kuttenn, F., Touraine, P., 2004. Significance of ovarian histology in the management of patients presenting a premature ovarian failure. Hum. Reprod. 19 (11) https://doi.org/10.1093/humrep/deh461.

McCarthy, D.J., Chen, Y., Smyth, G.K., 2012. Differential expression analysis of multifactor RNA-Seq experiments with respect to biological variation. Nucleic Acids Res. 40 (10) https://doi.org/10.1093/nar/gks042.

McCoy, J.A., Bangma, J.T., Reiner, J.L., Bowden, J.A., Schnorr, J., Slowey, M., O'Leary, T., Guillette, L.J., Parrott, B.B., 2017. Associations between perfluorinated alkyl acids in blood and ovarian follicular fluid and ovarian function in women undergoing assisted reproductive treatment. Sci. Total Environ. 605–606. https://doi.org/10.1016/j.scitotenv.2017.06.137.

Milnes, M.R., Guillette, L.J.J., 2008. Alligator Tales: new lessons about environmental contaminants from a sentinel species. Bioscience 58, 1027–1036.

Milnes, M.R., Allen, D., Bryan, T.A., Sedacca, C.D., Guillette Jr., L.J., 2004. Developmental effects of embryonic exposure to toxaphene in the American alligator (Alligator mississippiensis). Comp. Biochem. Physiol. 138, 81–87. C.

Milnes, M.R., Bryan, T.A., Medina, J.G., Gunderson, M.P., Guillette Jr., L.J., 2005. Developmental alterations as a result of in ovo exposure to the pesticide metabolite p,p'-DDE in Alligator mississippiensis. Gen. Comp. Endocrinol. 144 (3), 257–263.

Moore, B.C., Uribe-Aranzabal, M.C., Boggs, A.S.P., Guillette, L.J., 2008. Developmental morphology of the neonatal alligator (Alligator mississippiensis) ovary. J. Morphol. 269 (3), 302–312.

Moore, B.C., Hamlin, H.J., Botteri, N.L., Guillette Jr., L.J., 2010a. Gonadal mRNA expression levels of TGFbeta superfamily signaling factors correspond with post-hatching morphological development in American alligators. Sex Dev 4 (1–2), 62–72.

Moore, B.C., Hamlin, H.J., Botteri, N.L., Lawler, A.N., Mathavan, K.K., Guillette Jr., L.J., 2010b. Posthatching development of Alligator mississippiensis ovary and testis. J. Morphol. 271 (5), 580–595.

Moore, B.C., Kohno, S., Cook, R.W., Alvers, A.L., Hamlin, H.J., Woodruff, T.K., Guillette, L.J., 2010c. Altered sex hormone concentrations and gonadal mRNA expression levels of activin signaling factors in hatchling alligators from a contaminated Florida lake. J. Exp. Zool. Part A Ecol. Genet. Physiol 313 (4), 218–230. A.

Moore, B.C., Milnes, M.R., Kohno, S., Katsu, Y., Iguchi, T., Woodruff, T.K., Guillette, L.J., 2011. Altered gonadal expression of TGF-β superfamily signaling factors in environmental contaminant-exposed juvenile alligators. J. Steroid Biochem. Mol. Biol. 127 (1–2), 58–63.

Moore, B.C., Roark, A.M., Kohno, S., Hamlin, H.J., Guillette Jr., L.J., 2012a. Gene-environment interactions: the potential role of contaminants in somatic growth and the development of the reproductive system of the American alligator. Mol. Cell. Endocrinol. 354 (1–2), 111–120.

Moore, B.C., Forouhar, S., Kohno, S., Botteri, N.L., Hamlin, H.J., Guillette, L.J., 2012b. Gonadotropin-induced changes in oviducal mRNA expression levels of sex steroid hormone receptors and activin-related signaling factors in the alligator. Gen. Comp. Endocrinol. 175 (2), 251–258.

Pastore, L.M., Christianson, M.S., Stelling, J., Kearns, W.G., Segars, J.H., 2018. Reproductive ovarian testing and the alphabet soup of diagnoses: DOR, POI, POF, POR, and FOR. J. Assist. Reprod. Genet. 35 (1) https://doi.org/10.1007/s10815-017-1058-4.

Pertea, M., Pertea, G.M., Antonescu, C.M., Chang, T.C., Mendell, J.T., Salzberg, S.L., 2015. StringTie enables improved reconstruction of a transcriptome from RNA-seq reads. Nat. Biotechnol. 33 (3) https://doi.org/10.1038/nbt.3122.

Pertea, M., Kim, D., Pertea, G.M., Leek, J.T., Salzberg, S.L., 2016. Transcript-level expression analysis of RNA-seq experiments with HISAT, StringTie and Ballgown. Nat. Protoc. 11 (9) https://doi.org/10.1038/nprot.2016.095.

Pierron, F., Bureau Du Colombier, S., Moffett, A., Caron, A., Peluhet, L., Daffe, G., Lambert, P., Elie, P., Labadie, P., Budzinski, H., Dufour, S., Couture, P., Baudrimont, M., 2014. Abnormal ovarian DNA methylation programming during

gonad maturation in wild contaminated fish. Environ. Sci. Technol. 48 (19), 11688–11695.
Rauschenberger, R.H., Wiebe, J.J., Sepúlveda, M.S., Scarborough, J.E., Gross, T.S., 2007. Parental exposure to pesticides and poor clutch viability in American alligators. Environ. Sci. Technol. 41 (15), 5559–5563.
Rauschenberger, R.H., Sepúlveda, M.S., Wiebe, J.J., Wiebe, J.E., Honeyfield, D.C., Gross, T.S., 2009. Nutrient and organochlorine pesticide concentrations in American alligator eggs and their associations with clutch viability. J. Aquat. Anim. Health. https://doi.org/10.1577/H07-051.1.
Reimand, J., Arak, T., Adler, P., Kolberg, L., Reisberg, S., Peterson, H., Vilo, J. g, 2016. Profiler-a web server for functional interpretation of gene lists (2016 update). Nucleic Acids Res. 44 (W1) https://doi.org/10.1093/NAR/GKW199.
Richardson, M.C., Guo, M., Fauser, B.C.J.M., Macklon, N.S., 2014. Environmental and developmental origins of ovarian reserve. Hum. Reprod. Update 20 (3). https://doi.org/10.1093/humupd/dmt057.
Rivera, O.E., Varayoud, J., Rodríguez, H.A., Santamaría, C.G., Bosquiazzo, V.L., Osti, M., Belmonte, N.M., Muñoz-de-Toro, M., Luque, E.H., 2015. Neonatal exposure to xenoestrogens impairs the ovarian response to gonadotropin treatment in lambs. Reproduction 149 (6). https://doi.org/10.1530/REP-14-0567.
Robinson, M.D., Smyth, G.K., 2007. Moderated statistical tests for assessing differences in tag abundance. Bioinformatics 23 (21). https://doi.org/10.1093/bioinformatics/btm453.
Robinson, M.D., McCarthy, D.J., Smyth, G.K., edgeR, 2009. A Bioconductor package for differential expression analysis of digital gene expression data. Bioinformatics 26 (1). https://doi.org/10.1093/bioinformatics/btp616.
Roussigne, M., Kossida, S., Lavigne, A.C., Clouaire, T., Ecochard, V., Glories, A., Amalric, F., Girard, J.P., 2003. The THAP domain: a novel protein motif with similarity to the DNA-binding domain of P element transposase. Trends Biochem. Sci. 28 (2) https://doi.org/10.1016/S0968-0004(02)00013-0.
Seifert, B.A., Dejosez, M., Zwaka, T.P., 2017. Ronin influences the DNA damage response in pluripotent stem cells. Stem Cell Res. 23 https://doi.org/10.1016/j.scr.2017.06.014.
Soto, A.M., Chung, K.L., Sonnenschein, C., 1994. The pesticides endosulfan, toxaphene and dieldrin have estrogenic effects on human estrogen-sensitive cells. Environ. Health Perspect. 102, 380–383.
Trapnell, C., Williams, B.A., Pertea, G., Mortazavi, A., Kwan, G., Van Baren, M.J., Salzberg, S.L., Wold, B.J., Pachter, L., 2010. Transcript assembly and quantification by RNA-Seq reveals unannotated transcripts and isoform switching during cell differentiation. Nat. Biotechnol. 28 (5) https://doi.org/10.1038/nbt.1621.
Van Rooijen, E., Giles, R.H., Voest, E.E., Van Rooijen, C., Schulte-Merker, S., Van Eeden, F.J., 2008. LRRC50, a conserved ciliary protein implicated in polycystic kidney disease. J. Am. Soc. Nephrol. 19 (6) https://doi.org/10.1681/ASN.2007080917.
Vonier, P.M., Crain, D.A., McLachlan, J.A., Guillette, L.J., Arnold, S.F., 1996. Interaction of environmental chemicals with the estrogen and progesterone receptors from the oviduct of the American alligator. Environ. Health Perspect. 104 (12), 1318–1322.
Wesevich, V., Kellen, A.N., Pal, L., 2020. Recent advances in understanding primary ovarian insufficiency. F1000Research 9. https://doi.org/10.12688/f1000research.26423.1.
Windsor, F.M., Ormerod, S.J., Tyler, C.R., 2018. Endocrine disruption in aquatic systems: up-scaling research to address ecological consequences. Biol. Rev. 93 (1) https://doi.org/10.1111/brv.12360.
Xie, Z., Bailey, A., Kuleshov, M.V., Clarke, D.J.B., Evangelista, J.E., Jenkins, S.L., Lachmann, A., Wojciechowicz, M.L., Kropiwnicki, E., Jagodnik, K.M., Jeon, M., Ma'ayan, A., 2021. Gene set knowledge discovery with Enrichr. Curr. Protoc. 1 (3) https://doi.org/10.1002/cpz1.90.
Yilmaz, B., Terekeci, H., Sandal, S., Kelestimur, F., 2020. Endocrine disrupting chemicals: exposure, effects on human health, mechanism of action, models for testing and strategies for prevention. Rev. Endocr. Metab. Disord. 21 (1) https://doi.org/10.1007/s11154-019-09521-z.